

Choroidal metastasis resembling hemangioma on angiogram as initial manifestation of lung adenocarcinoma

Xin Liu, Jian Ma, Zhi-Tao Su, Li Zhang, Xiao-Yun Fang, Yao Wang

Eye Center of the 2nd Affiliated Hospital, School of Medicine, Zhejiang University, Hangzhou 310000, Zhejiang Province, China

Co-first authors: Xin Liu and Jian Ma

Correspondence to: Xiao-Yun Fang. Eye Center of the 2nd Affiliated Hospital, School of Medicine, Zhejiang University, No.88 Jiefang Road, Hangzhou 310000, Zhejiang Province, China. xiaoyunfangzju@163.com; Yao Wang. Eye Center of the 2nd Affiliated Hospital, School of Medicine, Zhejiang University, No.88 Jiefang Road, Hangzhou 310000, Zhejiang Province, China. wangyao@zju.edu.cn

Received: 2021-07-09 Accepted: 2022-01-25

DOI:10.18240/ijo.2022.07.23

Citation: Liu X, Ma J, Su ZT, Zhang L, Fang XY, Wang Y. Choroidal metastasis resembling hemangioma on angiogram as initial manifestation of lung adenocarcinoma. *Int J Ophthalmol* 2022;15(7):1203-1206

Dear Editor,

We present a case of choroidal metastasis (CM) masquerading as circumscribed choroidal hemangioma as initial manifestation of lung adenocarcinoma. The study procedures were in accordance with the Declaration of Helsinki and were approved by the Institutional Review Board of the Second Affiliated Hospital of Zhejiang University School of Medicine. Written informed consent was obtained from the patient.

A 61-year-old Chinese female came to the clinic and reported to have suffered from unilateral painless vision decrease with occasional floaters for 1mo. The patient denied discomfort during eye movement, amaurosis, double vision, dizziness, nor did she report any systemic symptom. She had been diagnosed with hypertension for 10y and with breast fibroadenoma for more than 1y.

Her visual acuities were 0.097 logarithm of the minimum angle of resolution (logMAR) for the right eye and 1.0 logMAR for the left one. Intraocular pressures were 17.3 mm Hg for the

right eye and 15.0 mm Hg for the left one. Anterior segment examination revealed shallow anterior chamber and mild lens opacity in both eyes. Ophthalmoscopic examination showed a prominent solid yellow-orange choroidal mass involving the macula in the left eye, with extensive subretinal fluid (SRF) ranging from the posterior pole to inferior retina. She failed to complete fundus photography examination due to her poor vision, so that scanning laser ophthalmoscopy (SLO) was applied to capture the lesion instead (Figure 1A). Scattered spots of pigment could also be observed on the surface of the mass (Figure 1A). No retinal abnormality was found in the right eye. B-scan ultrasound of the left eye demonstrated a smoothly elevated mass with homogeneously high internal reflectivity, and a crooked hyper-reflective line indicative of detached retina (Figure 1B). Significant elevation of retinal pigmented epithelium (RPE)/Bruch's membrane complex, caused by the large choroidal mass, prevented optical coherence tomography (OCT) from detailed recognition (Figure 1C). However, the altered structure of ellipsoid zone could be observed on OCT, and SRF was vaguely detected underneath the poorly-defined speckles-dotted RPE. Orbital enhanced magnetic resonance imaging (MRI) reported irregularly thickened posterior wall of the left eye (maximal thickness of 4.4 mm) that was hypointensive in both T1 (Figure 1D) and T2 (Figure 1E) weighted images, with suspicious enhancement (Figure 1F).

A week later, her visual acuity of the left eye decreased to finger count at 30 cm, and an exacerbation of retinal detachment was observed (Figure 2A). To ensure the safety of mydriasis before angiography, laser peripheral iridotomy (LPI) was carried out. Both fundus fluorescein angiography (FFA) and indocyanine green angiography (ICGA) showed irregular areas of hyper-fluorescence in the lesion during the early phase, which reflected a filling of intrinsic vascular architecture within the mass (Figure 2C, 2D). Scattered hyper-fluorescent pinpoint spots over the mass, blocked by patchy hypo-fluorescence, persisted in the venous phase and late phase (Figure 2E-2H). The hypo-fluorescent areas on FFA (Figure 2G) partially conformed to the pigment spots recognized by ophthalmoscopy (Figure 1A). According to the angiographic

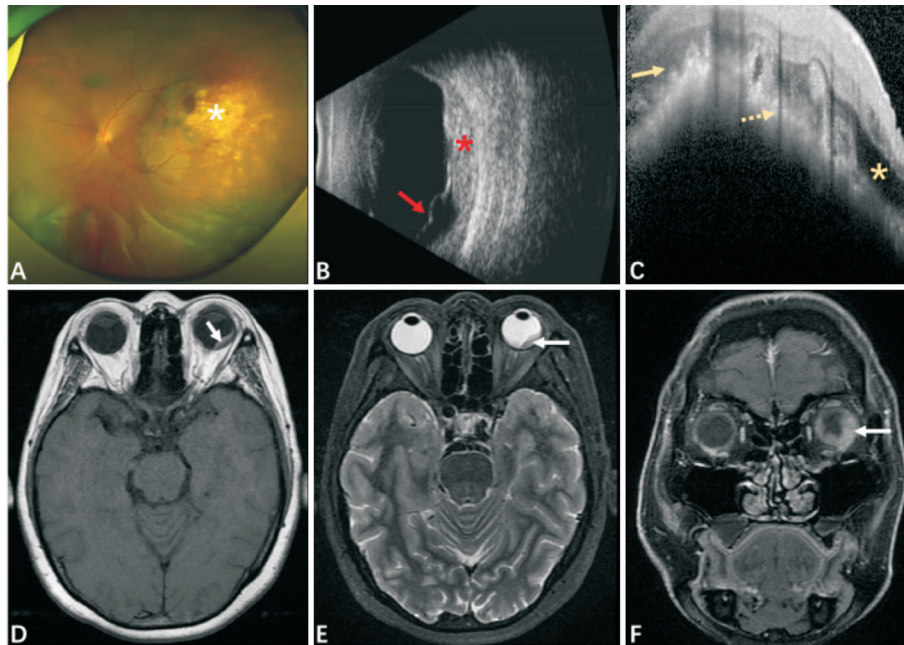


Figure 1 Clinical data of the left eye of the patient on her first visit The scanning laser ophthalmoscope photography (A) showed a yellow-orange lesion (white asterisk) involving the macula that extended temporally in the choroid, with associated exudative retinal detachment from the posterior pole to inferior retina and with spots of pigment accumulation. B-scan ultrasound (B) showed a smoothly elevated choroidal mass (red asterisk) with high and homogeneous internal reflectivity, and a crooked hyper-reflective line (red arrow) of retinal detachment that linked to the optic disc. Optical coherence tomography (C) showed obvious elevation of the entire choroid and retina, subretinal fluid (yellow asterisk), alterations of ellipsoid zone (yellow arrow), and hyper-reflective in RPE (yellow arrow with dashed line). In orbital enhanced MRI, irregularly thickened posterior wall of the left eye (maximal thickness of 4.4 mm) was displayed (white arrow) hypo-intense in both T1 (D) and T2 (E) weighted fat-suppression images, with suspicious localized enhancement (F). RPE: Retinal pigment epithelium; MRI: Magnetic resonance imaging.

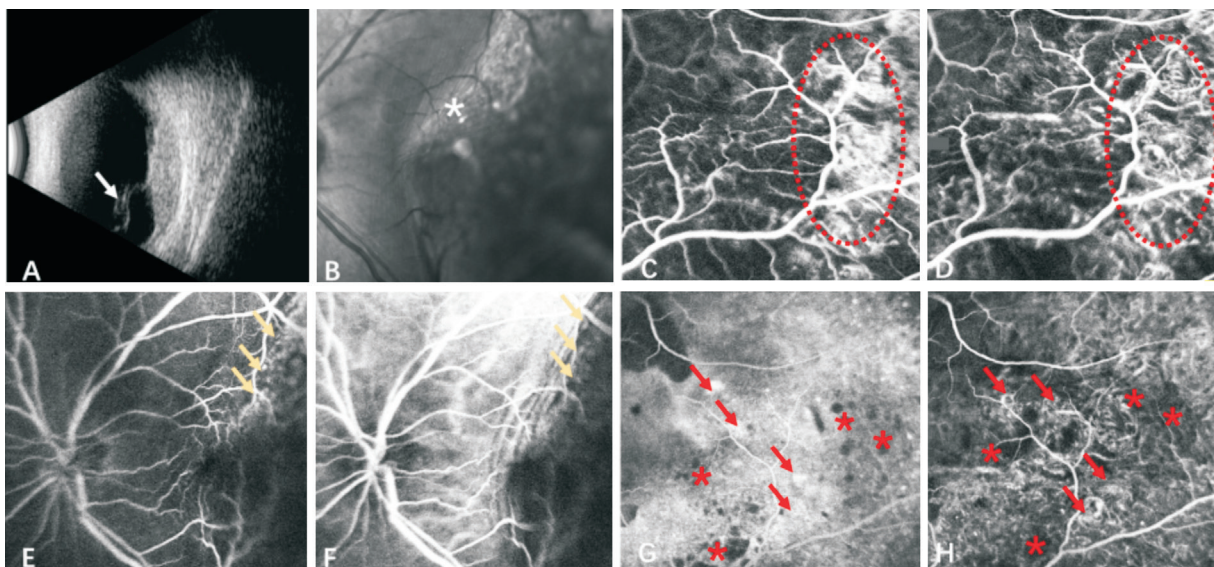


Figure 2 Clinical data of the left eye of the patient 1wk after her first visit In B-scan ultrasound (A), the mass revealed a dome-shaped appearance and the crooked hyper-reflective line of retinal detachment (white arrow) was more elevated. Infrared image (B) revealed a wrinkling of the choroid at the nasal border of the mass (white asterisk). FFA (C, E, G) and ICGA (D, F, H) at early (C, D, 26''), middle (E, F, 39'') and late (G, H, 8'35'') phase were presented. Detailed alterations of the central lesion site were interfered by the elevated retina (E, F). However, localized angiogram around the inferior margin of the mass indicated irregular areas of hyper-fluorescence (red dashed line) during the early phase (C, D), which reflected the filling of the intrinsic vascular architecture. Pinpoints of hyper-fluorescence (yellow arrows) could be detected around the superior margin of the mass (E, F) on both FFA and ICGA. Hyper-fluorescence persisted to the late phase (G, H) in an appearance of pinpoints (red arrows) with patches of blocked fluorescence due to pigment (red asterisks). FFA: Fundus fluorescein angiography; ICGA: Indocyanine green angiography.

manifestations, the clinician suspected circumscribed choroidal hemangioma, but advised further screening of malignancy considering her onset age and rapid progression.

In the following two weeks, the patient showed no clinically significant finding in abdominal ultrasound, abdominal enhanced computed tomography (CT), transvaginal ultrasound, breast ultrasound, and brain MRI. However, elevated levels of carcinoembryonic antigen (CEA, 8.6 ng/mL), cancer antigen-199 (CA-199, 86.7 U/mL), CA-211 (5.8 ng/mL), CA-125 (40.6 U/mL), CA-153 (123.6 U/mL), and neuron-specific enolase (NSE, 26.5 ng/mL), were detected in serum. More importantly, chest high resolution (HR)-CT revealed that a mass characterized of lobular and spiculate boundary, sized 35.1×37.6×33.1 mm³, was located on the left upper lobe. The patient was then admitted by oncology department for CT-guided lung puncture biopsy and radionuclide bone imaging. The biopsy results confirmed lung adenocarcinoma, showing positive for thyroid transcription factor-1 (TTF-1), cytokeratin 7 (CK7), and Napsin A, while negative for programmed death 1 ligand (PD-L1) and anaplastic lymphoma kinase-lung (ALK-lung) in immunohistochemistry. Genetic test indicated exon deletion mutation on epidermal growth factor receptor 19 (EGFR 19). Radionuclide bone imaging demonstrated multiple bone metastases. The patient was finally diagnosed with lung adenocarcinoma and began targeted therapy with gefitinib.

CM is considered the most common form of intraocular malignancy. However, the prevalence of symptomatic cases is reported to be less than 3%^[1]. Lung cancer was the primary cancer site of CM in 21% cases, accounting 40% cases of males and 12% cases of female^[2]. A Meta-analysis of CM from lung malignancy reported that 42% were adenocarcinomas^[3]. Among choroidal masses, choroidal metastases present highly various clinical manifestations^[4]. Therefore, differential diagnosis of CM from other choroidal masses was important for prompt systemic evaluation. Both CM and choroidal hemangioma could display yellow-orange mass on fundoscopic examination, and are frequently associated with wide range of exudative retinal detachment. Spots of pigment accumulation are also common signs of both diseases. In this case, the main challenges for diagnosis are as follows: first, the morphology and reflectivity distribution on B-scan ultrasound were not typical of CM; second, a wide range of elevated retina caused by exudative retinal detachment interfered with clear structure detection in OCT and FFA/ICGA; most importantly, the relatively rich blood supply of the choroidal mass, reflected by FFA/ICGA and MRI enhancement, complicated the diagnosis process, for it accorded with the characteristics of circumscribed choroidal hemangioma rather than those of common CM^[5]. Choroidal tuberculoma, nevertheless, could displayed various characteristics which can be delusive, and

should be addressed in areas with heavy burden of tuberculosis patients. Yellow-orange lesion with exudative retinal detachment could be observed in some cases^[6], but would mostly accompany other features of uveitis^[7]. A lack of anterior uveitis, insufficient evidence of lung tuberculosis, and biopsy result could decrease the possibility of tuberculosis, although a specific lab examination on *Mycobacterium tuberculosis* would be more convincing.

B-scan ultrasound is an important screening method to assess choroidal masses. Typical CMs on B-scan ultrasound would show multilobular flat or dome-shaped masses of heterogeneous reflectivity with irregular surface^[4]. Circumscribed choroidal hemangioma, on the other hand, is characteristic of a slightly dome-shaped mass with homogeneous hyper-reflectivity internally and with acoustic solidity similar to the surrounding choroid^[5]. In our case, although the slightly elevated morphology of the mass could indicate both CM and hemangioma, the solitary lesion, the smooth surface and the generally homogeneous reflectivity favored the diagnosis of circumscribed choroidal hemangioma. In OCT, the lesion of CM would appear to be lumpy bumpy with alterations in RPE and morphological changes in photoreceptors^[4], while choroidal circumscribed hemangioma mostly would appear as a distinct elevation with smooth surface delimited from choriocapillaris interface^[8]. Although the OCT images of our patient were greatly influenced by the extensive retinal detachment, the obvious alterations of RPE supported the diagnosis of CM.

As for angiography, ICGA outweighs FFA in the differential importance of choroidal masses. Classic features of CM in FFA should be hypo-fluorescent in the early phase and heterogeneously hyper-fluorescent in the late phase. However, sometimes the FFA of CM is hyper-fluorescent at all phases, leading to a misdiagnosis of hemangioma^[9]. ICGA pattern of CM, on the other hand, is usually defined as hypo-fluorescent at all phases on an underlying iso-fluorescent background^[4]. Compared to FFA, the mottled hyper-fluorescence of the mass in the late phase is seldom described in ICGA. Even in a case report that misdiagnosed CM for hemangioma while presented ICGA result, ICGA still appeared hypo-fluorescent^[10]. In circumscribed choroidal hemangioma, the angiogram is intense and achieves rapid hyper-fluorescence in both FFA and ICGA due to its rich intrinsic vasculature^[11]. Therefore, the hyper-fluorescent feature in FFA and ICGA of our patient favored the diagnosis of circumscribed choroidal hemangioma instead of CM.

Previous studies showed that CMs were iso-intense on T1-weighted images and hypo-intense on T2-weighted images, while choroidal hemangiomas were hyper-intense on T1-weighted images and iso-intense on T2-weighted images^[12].

After enhancement, CMs generally show bright signal on T1-weighted and low signal on T2-weighted images, while choroidal hemangiomas show bright signal on both T1- and T2-weighted images. Orbital MRI of our patient displayed hypo-intense signals on both T1- and T2-weighted images, which might suggest metastasis. Nonetheless, localized enhancement detected on T2-weighted images tended to indicate hemangioma.

In summary, unusual pattern of a smooth morphology and a relatively rich vascularization could be detected in CMs. Multimodal imaging examinations as well as appropriate systemic screening are necessary in diagnosing choroidal masses.

ACKNOWLEDGEMENTS

Authors' contributions: Wang Y performed the initial and follow-up visits, evaluated clinical data, and revised the manuscript. Liu X assembled the data and was a major contributor in writing the manuscript. Ma J was also a contributor in writing the manuscript. Su ZT assisted in literature review. Zhang L and Fang XY reviewed the manuscript. The authors read and approved the final manuscript.

Foundation: Supported by Medical Scientific Research Foundation of Zhejiang Province, China (No.201130184).

Conflicts of Interest: Liu X, None; Ma J, None; Su ZT, None; Zhang L, None; Fang XY, None; Wang Y, None.

REFERENCES

- 1 Mariachiara M, Celeste R, Federico F, Nicole B, Antonio C. Choroidal metastasis from non-small-cell lung cancer responsive to Osimertinib: a case report. *Int Ophthalmol* 2018;38(6):2669-2675.
- 2 Ye XM, Kaliki S, Shields CL. Rapid regression of choroidal metastasis from lung cancer using erlotinib (Tarceva). *Oman J Ophthalmol* 2014;7(2):75-77.
- 3 Funazo T, Morita K, Ikegami N, *et al.* Successful treatment with alectinib for choroidal metastasis in anaplastic lymphoma kinase rearranged non-small cell lung cancer. *Intern Med* 2017;56(17):2317-2320.
- 4 Mathis T, Jardel P, Loria O, Delaunay B, Nguyen AM, Lanza F, Mosci C, Caujolle JP, Kodjikian L, Thariat J. New concepts in the diagnosis and management of choroidal metastases. *Prog Retin Eye Res* 2019;68:144-176.
- 5 Sen M, Honavar SG. Circumscribed choroidal hemangioma: an overview of clinical manifestation, diagnosis and management. *Indian J Ophthalmol* 2019;67(12):1965-1973.
- 6 Young L, Yakin M, Sen HN. Choroidal granuloma resolution with tuberculosis treatment. *Am J Ophthalmol Case Rep* 2020;20:100969.
- 7 Shahidatul-Adha M, Zunaina E, Liza-Sharmini AT, Wan-Hazabbah WH, Shatriah I, Mohtar I, Azhany Y, Adil H. Ocular tuberculosis in Hospital Universiti Sains Malaysia-a case series. *Ann Med Surg (Lond)* 2017;24:25-30.
- 8 Filloy A, Caminal JM, Arias L, Jordán S, Català J. Swept source optical coherence tomography imaging of a series of choroidal tumours. *Can J Ophthalmol* 2015;50(3):242-248.
- 9 Papastefanou VP, Arora AK, Hungerford JL, Cohen VML. Choroidal metastasis from follicular cell thyroid carcinoma masquerading as circumscribed choroidal haemangioma. *Case Rep Oncol Med* 2014;2014:251817.
- 10 Leahy KE, Karaconji T, Thanni V, Achan A, Fung AT. Metastatic small-cell neuroendocrine carcinoma simulating circumscribed choroidal hemangioma. *Ocul Oncol Pathol* 2015;2(1):13-15.
- 11 Mashayekhi A, Shields CL. Circumscribed choroidal hemangioma. *Curr Opin Ophthalmol* 2003;14(3):142-149.
- 12 Peyster RG, Augsburger JJ, Shields JA, Hershey BL, Eagle R Jr, Haskin ME. Intraocular tumors: evaluation with MR imaging. *Radiology* 1988;168(3):773-779.